Science of the Total Environment 912 (2024) 169303

Contents lists available at ScienceDirect

Science of the Total Environment

journal homepage: www.elsevier.com/locate/scitotenv

The probiotic SLAB51 as agent to counteract BPA toxicity on zebrafish gut microbiota -liver-brain axis

Christian Giommi [a,b,1], Marta Lombó [a,b,c,1], Hamid R. Habibi [e], Giacomo Rossi [d], Danilo Basili [a], Sara Mangiaterra [d], Claudia Ladisa [e], Giulia Chemello [a,b], Oliana Carnevali [a,b,*], Francesca Maradonna [a,b]

[a] Dipartimento Scienze della Vita e dell'Ambiente, Università Politecnica delle Marche, Via Brecce Bianche, 60131 Ancona, Italy
[b] INBB - Consorzio Interuniversitario di Biosistemi e Biostrutture, 00136 Roma, Italy
[c] Department of Molecular Biology, Faculty of Biology and Environmental Sciences, Universidad de León, 24071 León, Spain
[d] School of Biosciences and Veterinary Medicine, University of Camerino, 62024 Matelica (MC), Italy
[e] Department of Biological Sciences, University of Calgary, Calgary, Alberta T2N 1N4, Canada

HIGHLIGHTS

- SLAB51 mitigates BPA-induced toxicity at gut, brain, liver and spleen levels.
- SLAB51 counteracts the alterations triggered by BPA on gut architecture.
- SLAB51alleviates BPA-induced gut dysbiosis, enhancing the immune response.
- SLAB51 mitigates BPA hepatotoxicity by restoring glycogen and lipids levels.
- SLAB51 mitigates BPA neurotoxicity.

GRAPHICAL ABSTRACT

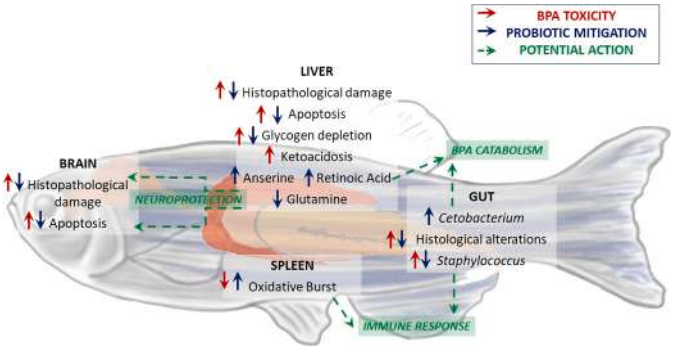

ARTICLE INFO

Editor: Henner Hollert

Keywords:
Endocrine disruptors, metabolomics
Histology
Immunohistochemistry
Probiotics
Immune system

ABSTRACT

A plethora of studies have so far described the toxic effects of bisphenol A (BPA) on organism health, highlighting the urgent need to find new strategies not only to reduce the presence of this toxicant but also to counteract its adverse effects. In this context, probiotics emerged as a potential tool since they promote organism welfare. Using a multidisciplinary approach, this study explores the effects of SLAB51 dietary administration to counteract BPA toxicity using zebrafish as a model. Adult males and females were maintained under standard conditions (control group; C), exposed for 28 days *via* the water to an environmental relevant dose of BPA (10 μg/L; BPA), dietary treated with SLAB51 (10^9 CFU/g of body weight; P) and co-treated with BPA plus SLAB51 (BPA + P). In the gut, exposure to BPA resulted in altered architecture in both males and females, with females also experiencing an increase of pathogenic bacterial species. Co-administration of BPA + P led to the restoration of

* Corresponding author at: Dipartimento Scienze della Vita e dell'Ambiente, Università Politecnica delle Marche, Via Brecce Bianche, 60131 Ancona, Italy.
E-mail addresses: c.giommi@pm.univpm.it (C. Giommi), mloma@unileon.es (M. Lombó), habibi@ucalgary.ca (H.R. Habibi), giacomo.rossi@unicam.it (G. Rossi), sara.mangiaterra@unicam.it (S. Mangiaterra), cladisa@verschurencentre.ca (C. Ladisa), g.chemello@staff.univpm.it (G. Chemello), o.carnevali@staff.univpm.it (O. Carnevali), f.maradonna@univpm.it (F. Maradonna).
[1] The Authors equally contributed.

https://doi.org/10.1016/j.scitotenv.2023.169303
Received 3 October 2023; Received in revised form 5 December 2023; Accepted 10 December 2023
Available online 20 December 2023

normal gut architecture, favored beneficial bacteria colonization, and decreased the abundance of pathogenic species. In the liver, male BPA exposure led to steatosis and glycogen depletion, which was partially mitigated by SLAB51 co-administration. In contrast, in females exposed to BPA, the lack of steatosis along with the greater glycogen depletion, suggested an increase in energy demand as supported by the metabolomic phenotype. The analysis of liver metabolites in BPA + P males revealed increased levels of anserine and reduced levels of glutamine, which could lie behind the counteraction of the brain histopathological damage caused by BPA. In BPA + P females, a reduction of retinoic acid was found in the liver, suggesting an increase in retinoids responsible for BPA detoxification. Overall, these results demonstrate that SLAB51 exerts its beneficial effects on the gut microbiota-brain-liver axis through distinct molecular pathways, effectively mitigating the pleiotropic toxicity of BPA.

1. Introduction

The bidirectional interaction among the gut and its microbiota, the liver, and the central nervous system (CNS) is known as the gut microbiota-liver-brain axis. Indeed, the intestinal microbiota influences not only gut homeostasis but also other organs inside and outside the digestive system, such as liver and brain (Long-Smith et al., 2020; Tripathi et al., 2018). The communication between the gut and the CNS involves the autonomic nervous system, the neuroendocrine system, the hypothalamic-pituitary-adrenal axis, the immune system, and metabolic pathways (Cryan et al., 2019). On the other hand, the gut and the liver directly communicate *via* the portal vein, therefore all absorbed nutrients and factors coming from the gut, such as bacterial metabolites as well as toxins end up in the liver, where they are metabolized. Moreover, the liver stores glycogen, converts byproducts, such as ammonia into urea (Milosevic et al., 2019), and produces bile to digest fat. Interestingly, current research studies correlated the alterations of gut microbial communities with both neurological (neuropsychiatric and neurodegenerative ones) (Morais et al., 2021) and liver disorders (steatosis and inflammation) (Manzoor et al., 2022).

One of the factors contributing to gut dysbiosis is the exposure to several contaminants that, being ubiquitously distributed in the environment, can enter the organism *via* different ways, such as digestive, respiratory, and dermal contact (Ma et al., 2019). Noteworthy, emerging evidence has proven the causal relationship among contaminant exposure, gut dysbiosis, and alterations in the gut-liver-brain axis (Matsuzaki et al., 2023; Shi et al., 2022). In that regard, bisphenol A (BPA), which is essential for the manufacturing of polycarbonate plastics, epoxy resins, and many plastic products, has been one of the most studied (European Food Safety Authority, EFSA, 2023). Hence, mice dietary exposure to BPA has been demonstrated to disrupt both gut and blood-brain barriers and to change the gut microbial community, being these effects much more severe in males, which showed a remarkable cognitive impairment (Ni et al., 2021). Concerning the gut-liver axis, male mice exposed to BPA displayed gut dysbiosis, altered intestinal barrier, and increased serum lipopolysaccharide levels, leading to hepatic inflammation (Feng et al., 2020). In zebrafish, chronic exposure to BPA (0.2 and 20 μg/L), alone and in combination with nano TiO_2, has been reported to shift gut microbiota, modify neurotransmission throughout the brain-gut-microbiota axis, disrupted the permeability of the intestinal barrier, and altered the inflammatory response and oxidative gut homeostasis (Chen et al., 2018). Embryonic exposure to 0.5 μg/L BPA for 60 days induced gut-brain transcriptional alterations accompanied by brain histological injury, microglia activation, enhanced apoptosis, and neuron loss in brain (Mu et al., 2023). As for the hepatic toxicity, in zebrafish, exposure to 15 μg/L BPA during the first three months of development led to sex-dependent disruptive effects on liver lipid metabolism (Zhu et al., 2023). Likewise, in the same species, adult female exposure to 20 μg/L BPA increased the lipid vacuole content in the hepatic tissue (Forner-Piquer et al., 2018).

Given the described toxicity of BPA, the European Community imposed significant restrictions on its use since the early 2000s Regulation (EU) 2016/1011, 2016. Moreover, based on the data available and the current knowledge, the EFSA has reduced the tolerable daily intake for BPA from 4 μg/kg body weight per day to 0.2 ng/kg body weight per day (Lambré et al., 2023). Despite the implementations of these and other measures to reduce human and animal exposure to BPA, new strategies to mitigate its toxicity are developing, especially those targeting reproduction, such as the use of natural compounds (resveratrol and epigallocatechin gallate) (Bordbar et al., 2023; Lombó and Herráez, 2021) and probiotics (Giommi et al., 2021). "Probiotics are living microorganisms that, when administered in adequate amounts, confer health benefits on the host" (Dahiya and Nigam, 2022). Hitherto, several studies have already demonstrated the potential of probiotics to counteract the harmful effects of contaminants. In rats, *Bifidobacterium breve* and *Lactobacillus casei* reduced the intestinal absorption of orally administered BPA (Oishi et al., 2008), whereas in zebrafish, *L. rhamnosus* antagonized perfluorobutanesulfonate (PFBS) metabolic (Chen et al., 2020; Hu et al., 2021; Liu et al., 2021) and neurological toxicity (Liu et al., 2020). In addition, *L. plantarum ST-III* reduced the proinflammatory actions of triclosan in zebrafish (Zang et al., 2019). Recently, results obtained in our laboratory using zebrafish demonstrated that the probiotic mixture used in this study, SLAB51, mitigates BPA-induced reproductive toxicity (Giommi et al., 2021). As regards to SLAB51 (commercially sold as SivoMixx®), it is a mixture of lactic acid bacteria and bifidobacteria that has been shown to exert neuroprotective effects in an Alzheimer's disease mice model (Bonfili et al., 2018) and to improve intestinal health in different animal species (Desantis et al., 2019; Mangiaterra et al., 2022; Rossi et al., 2020).

In this scenario, the hypothesis of the present study is that SLAB51 administration could mitigate the toxicity induced by chronic exposure to an environmentally relevant concentration of BPA on zebrafish homeostasis. The objective of this study is to deepen the understanding of the pleiotropic toxicity of BPA, which may alter the microbiota gut-liver–brain-axis. For this purpose, we have employed a multidisciplinary approach combining evidence from histopathological and immunohistopathological assays as well as metagenomic and metabolomic analyses in both male and female zebrafish. Additionally, we aim to analyze the potential beneficial effects of probiotics on mitigating these harmful effects and restoring the overall organism health.

2. Materials and methods

2.1. SLAB51 probiotic mix

The commercial multi-strain probiotic SLAB51 (SivoMixx®, Ormendes SA, Jouxtens-Mézery, CH, Switzerland) contains eight lyophilized bacteria strains: *Streptococcus thermophilus* DSM 32245 (80 billion CFU); *B. lactis* DSM 32246 (25 billion CFU); *B. lactis* DSM 32247 (25 billion CFU); *L. acidophilus* DSM 32241 (5 billion CFU); *L. helveticus* DSM 32242 (1 billion CFU); *L. paracasei* DSM 32243 (12 billion CFU); *L. plantarum* DSM 32244 (16 billion CFU); *L. brevis* DSM 27961 (36 billion CFU), at a total concentration of 2×10^{11} CFU/g.

2.2. Fish maintenance

A total of 176 (88 females and 88 males) six-month-old wild type zebrafish (AB strain, *Danio rerio*), with similar sizes and without

observable abnormalities, were randomly selected from the facility and maintained in glass tanks with oxygenated water under controlled conditions (28.0 ± 0.5 °C and 14/10 h of light/dark photoperiod). The chemical-physical parameters of the water were constantly monitored. Experimental fish were daily fed with a quantity of dry food (TetraMin Granules; Tetra, Melle, Germany) ranging from 2.5 to 3.0 % of body weight in the morning and *Artemia salina* in the afternoon.

The experiments were conducted in duplicate using 30-L glass tanks in a semi static system. Adult fish, 44 females and 44 males, were equally divided in four experimental groups: control (C) group, fed with commercial dry food as described above; probiotic (P) group, fed with commercial dry food enriched with the lyophilized probiotic SLAB51 at a final concentration of 10^9 CFU/g body weight; BPA group, fed with commercial dry food and exposed to 10 μg/L BPA (98 % analytical purity, Sigma-Aldrich, Milan, Italy) *via* water; BPA and SLAB51 (BPA + P) group, fed with commercial dry food enriched with the same concentration of SLAB51 mentioned above and exposed to 10 μg/L BPA *via* water. This dose of BPA was selected considering previous studies reporting its ability to alter liver metabolism (Forner-Piquer et al., 2018), whereas the SLAB51 concentration was selected based on previous studies in mice (Castelli et al., 2020; Cuozzo et al., 2021) and zebrafish (Giommi et al., 2021).

The experiment was conducted in accordance with the University of Calgary animal care protocol (AC15–0183) for the care and the use of experimental animals. All efforts were made to minimize suffering during all procedures involving animals, and no deaths were registered during the treatments in any experimental group. After 28 days of treatment, fish were euthanized using an excess of MS-222 (3-aminobenzoic acid ethyl ester; Merck, Darmstat, Germany) buffered to pH 7.4, according to University of Calgary animal care protocol for the care and the use of experimental animals.

2.3. Histological analysis of gut

The gut histological analysis was conducted on 6 females and 6 males per each experimental group. Zebrafish gut was harvested from the fish by stapling it in the esophagus and in the anus and cut it out as an entire portion. After 2-h fixation in 4 % paraformaldehyde (PFA) in 0.1 M phosphate buffer (PBS), pH 7.4, at room temperature (RT), samples were washed and stored in PBS. The zebrafish whole gut was then paraffin embedded by placing it inside a molding cassette and 4 μm histological sections of the gut were obtained using Leica RM2125 RTS rotating microtome (Leica, Wetzlar, Germany) and stained with Hematoxylin and Eosin to analyze intestinal fold length, thickness of lamina propria, basal lamina, and smooth muscle. Alcian blue staining (Bio-Optica, Milan, Italy) of acid mucins was also performed to assess the presence and the number of goblet cells per 100 μm of intestinal fold length. All the analyses were performed in the mid gut portion in a blind fashion of 5 random fields at 200× and 400× magnification for each sample. The representative microphotographs of each treatment in both staining at 200× and 400× magnification are shown in Supplementary Fig. 1.

2.4. Histopathological evaluation of liver and brain

To evaluate the histopathological status at hepatic and neurological level, livers ($n = 3$ for each experimental group) and brains ($n = 6$ for C females, C males, BPA females, BPA males, BPA + P male and P males, $n = 4$ for P females and $n = 8$ for BPA + P females) were fixed for 2 h at RT with 4 % PFA in 0.1 M PBS, pH 7.4, and then washed and stored in PBS solution until paraffin embedded. 3 μm-section of brain samples were cut on Leica RM2125 RTS rotating microtome (Leica, Wetzlar, Germany) and stained with Hematoxylin and Eosin for injury scoring.

A Periodic Acid Shift (PAS) staining (Bio Optica, Milan, Italy) was conducted on 3 μm-sections following the manufacturer's instructions for injury scoring and analysis of glycogen presence. Liver injury was assessed through blind histopathological evaluation of 5 random sections at 400× magnification, assigning a score for each sample based on the criteria reported in Supplementary Table 1. Hepatocyte vacuolar degeneration was used to assess the swollen aspect of the cells, steatosis (from microvesicular steatosis to diffuse form), cellular ballooning degeneration (none, few balloon cells, many cells, and prominent/diffuse ballooning degeneration), and degree of fibrosis. The score is represented as (−) absence, (+) mild, (++) moderate, and (+++) severe, and entails the localization of the degenerative process (Zone 3, Zone 2/1, Azonal, and Pan-Acinar/Lobular diffusion), and the percentage of parenchyma involvement (<5 %; 5 %–33 %; 33 %–66 %; >66 %). In Supplementary Fig. 2, representative microphotographs of different degrees of liver injury are reported.

Brain injury was assessed through blind histopathological evaluation of 5 random sections at 600× magnification, assigning a score for each section based on the criteria reported in Supplementary Table 2. Scoring analysis was performed on uniform brain sections, with grading done on two regions: hippocampus, and the mid-thalamus. Analysis was performed in a blinded fashion and regions were scored as follows: (−) absence, (+) mild, (++) moderate, and (+++) severe.

In both liver and brain, the score observed in at least 50 % of samples was indicated as representative of the group. In Supplementary Fig. 3, representative microphotographs of different degrees of brain injury are reported.

2.5. TUNEL assay in brain and liver

To analyze the apoptosis in both liver and brain, the same paraffin-embedded samples used for histopathological analysis were processed following the TUNEL technique using an *in-situ* apoptosis detection kit (PROMEGA Corporation, Madison, Wisconsin, USA) according to the manufacturer's instructions. The sections were counterstained with Mayer's Hematoxylin and the apoptotic nuclei displaying a dark brown color. Positive and negative control sections were included in each sample as follow: for a positive control, the same tissue sections were used but treated with 200 ng/ml DNAse I to introduce DNA breaks in all nuclei. For this purpose, adjacent sections were incubated with DNAse I for 1 h at 37ºC before to perform the test. For a negative control, TdT enzyme from the labeling mix was omitted. The data were expressed as the number of apoptotic cells counted in 5 randomly selected fields evaluated at 200× magnification for liver and 600× magnification for brain.

2.6. Brain GFAP and TAU aggregates immunoreaction

Glial fibrillary acidic protein (GFAP) and microglia antibodies have been used as markers for axonal damage, reactive astrocytes and activated microglia, respectively. The GFAP-immunoreaction (GFAP-IR) method was performed on the same brain samples of histopathology following the protocol previously described by Sriram et al. (2004) with slight modifications and conducted in different areas of the hippocampal formation.

Pathological inclusions in neurons and glial cells containing fibrillary aggregates of TAU protein are characteristic features in tauopathies and in some degenerative CNS diseases, also of toxic origin (Waheed et al., 2023). Brain sections of the same samples used for histopathology were deparaffinized and pre-treated with primary antibody [Anti-Tau antibody 1:400 (ab64193, Abcam)] to evaluate diffuse extra-neuronal neurofibrillary tangles (sparsely stained) and/or intra-neuronal (in neuropil) or intra-glial aggregates. Sections were then incubated at 4 °C overnight. Binding was detected with biotinylated anti-mouse or rabbit secondary antibody (BA-2000, Vector Laboratories) and developed with Vectastain ABC kit (PK-6100, Vector Laboratories), after a 45 min of incubation with ABC solution, then diaminobenzidine hydrochloride (DAB, SK-4105 Vector Laboratories) for 5 min. Tissues were counterstained with Mayer's hematoxylin, then dehydrated in a series of ethanol (70–100 %) and xylene, and coverslip was mounted with Poly-

Mount xylene (Polysciences, Inc. USA). For both immunohistochemistry reaction, positive cells were counted in 5 randomly selected fields at 600× for each sample.

2.7. Spleen respiratory burst assay

Respiratory burst assay protocol was performed as described by Graham and Secombes (1990), with subtle modifications, on 3 pools of 8 spleen each for each experimental group for both females and males. To count the nuclei an incubation with basic media was performed at room temperature for 15 min. Then the media was removed and two washes with 70 % MeOH were performed. At the end, the 70 % MeOH was removed, and wells were then air dried. 120 μL of KOH and 140 μL DMSO were then added in each well and mixed in microplate reader (Tecan Sunrise or GloMax Multi+, Promega) and the absorbance was read at 620-630 nm.

2.8. Metabolite extraction and UHPLC-ESI-MS analysis

Liver metabolite extraction, separation, and identification were performed as described previously (Giommi et al., 2021; Ladisa et al., 2021). Metabolites were extracted from pools of at least 3 livers with a final weight of ~25 mg per pool, being a total of 6 pools from females and 4 pools from males in both BPA and P groups, and 5 pools from females and 4 from males for both BPA + P and C groups. A quality control group (QC, $n = 5$) was generated by pooling random samples to investigate the presence of outliers and assess the dataset reliability as described previously.

MetaboAnalyst 5.0 online platform (University of Alberta, Alberta, Canada) was used to perform unsupervised Principal Component Analysis (PCA) on all treatments and QC to identify potential outliers and assess the LC-MS reliability. In addition, PLS-DA analysis was performed, and quality assessment of the models was indicated by R2 and Q2 > 0.5 (Giommi et al., 2021; Ladisa et al., 2021). Univariate analysis was performed using multiple *t*-tests on metabolites with VIP (Variable Importance in Projection) score > 1 of each model, using Metaboanalyst 5.0 as described previously. A significant threshold of *P* value adjusted using False Discovery Rate (FDR) < 0.05 was used to assess statistically significant differences among experimental groups. Metabolites with VIP score > 1 in each PLS-DA model were used to perform Pathway Analysis (MetPA) using Metaboanalyst 5.0 platform (Giommi et al., 2021; Ladisa et al., 2021). This technique considers the concentration of each metabolite, using Quantitative Enrichment Analysis (QEA) and the position in the pathway using Topological Analysis. For these two parameters, global test and relative-betweenness centrality algorithms were selected using the KEGG pathway library of zebrafish (*D. rerio*) as a reference.

2.9. DNA extraction, PCR and Marker gene (16S) amplicon sequencing and OTU assignments

Total DNA was extracted from gut samples (6 females and 6 males from C group and 3 females and 3 males from BPA, BPA + P and P groups), using the DNeasy Blood & Tissue Kits (Qiagen, Milan, Italy). A PCR amplification step was performed to amplify the V4 and V3 variable regions of the 16S rRNA gene using Illumina adapted primer 341F (CCTACGGGNGGCWGCAG), and Illumina adapted barcoded 805R primer (GACTACHVGGGTATCTAATCC) following 16S metagenomic sequencing library preparation protocol (Illumina, San Diego, CA). Samples and final libraries were quantified, and quality tested using the Qubit 2.0 fluorometer (Invitrogen, Carlsbad, CA). Additionally, libraries were quality checked on Agilent 2100 bioanalyzer (Agilent Technologies, Santa Clara, CA). Finally, amplicons were sequenced on the Illumina MiSeq platform run in paired-end mode with 300-bp read length by IGA Technology Services (www.igatechnology.com).

Demultiplexing was performed with CASAVA v. 1.8 and reads not matching indexes or representing the PhiX were removed. Raw sequence reads were processed with the Python package Cut Adapt v1.4.2 to remove any residual adapter contamination, and quality trimming of paired-end reads was performed using the erne-filter command (Erne v1.4.6, default parameters except min-size = 200). Reads with a minimum length of 200 bp were retained and analyzed with QIIME v1. Briefly, the USEARCH (v8.1.1756, 32-bit) quality filter pipeline was employed to filter chimeric reads, group replicate sequences, sort sequences per decreasing abundance, and identify OTUs. OTU picking was achieved by applying a minimum pairwise identity threshold of 97 %. The most abundant sequence in each OTU was selected to assign a taxonomic classification based on the Greengenes database (v 2013_5) using the RDP classifier (v2.2), clustering the sequences at 97 % similarity with a 0.50 confidence threshold. Outliers and singletons were then removed before running downstream analysis.

2.10. Statistical analysis

Microbiota data analysis was performed within the R statistical environment. Quality control was performed to identify potential outliers as well as to ensure a good level of similarity between replicates. In order to perform diversity analysis, a data normalization relying on scaling with ranked subsampling (SRS) was applied using the R package SRS (Beule and Karlovsky, 2020). The R package Phyloseq was used for diversity estimates where Shannon, Simpson and Observed species were used as diversity indexes (McMurdie and Holmes, 2013). Statistical differences in alpha diversity were assessed by using either the ANOVA followed by Tukey HSD post-hoc test or the Kruskal-Wallis test followed by the Wilcoxon pairwise post-hoc test, depending on normality and sample variance assumptions. The Benjamini-Hochberg FDR correction was applied. The ADONIS function based on Bray-Curtis distances (R vegan package) was used to analyze community composition. Bar-plots of microbial abundances were drawn firstly taking the average of replicates and then considering taxa whose total abundance across all samples was at least 1 %. Differential analysis was performed using raw counts as input into DESeq2 and considering a 5 % FDR threshold (Love et al., 2014). Functional profiles for 16S rRNA gene sequence data were predicted using the Phylogenetic Investigation of Communities by Reconstruction of Unobserved States (PICRUSt2) (Caicedo et al., 2020) and analyzed using the Linear discriminant analysis Effect Size (LEfSe) within Galaxy (Jalili et al., 2021; Segata et al., 2011).

One-Way ANOVA followed by Dunnett's multiple comparison test was used for gut histopathology, TUNEL assay, GFAP and TAU quantification, and Burst Respiratory data. Statistical software package Prism 8 (GraphPad Software, Inc., San Diego, CA, USA) was used to perform statistical analyses with significance accepted at $P < 0.05$.

3. Results

3.1. Analysis of gut architecture

The histological analysis of the gut revealed a decrease in the height of the intestinal folds and an increase in the thickness of the intestinal lamina propria in both females and males exposed to BPA. However, these alterations in gut structure were no longer found in the BPA-exposed fish co-treated with probiotic (Fig. 1 a,b,f,g). Even though no changes among groups were observed regarding the thickness of intestinal basal lamina (Fig. 1 c,h), the exposure to BPA caused a reduction of males intestinal muscle thickness when compared to BPA + P group, while no changes in females were reported (Fig. 1 d,i). The Alcian Blue staining just showed an increase in the number of goblet cells in the BPA-exposed males co-treated with SLAB51 when compared to both C and BPA-exposed males (Fig. 1 e,j).

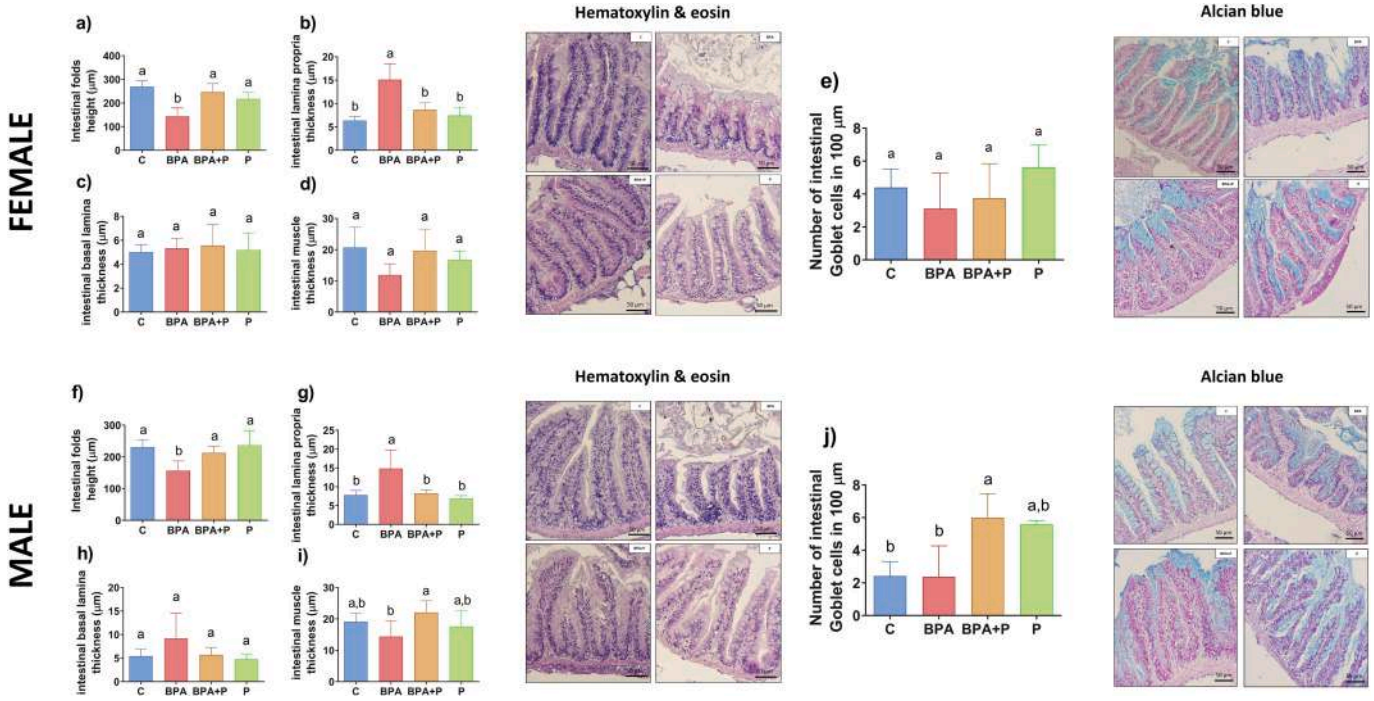

Fig. 1. Histological evaluation of gut samples. a,f) Intestinal Fold Height (μm), b,g) Intestinal Lamina Propria Thickness (μm), c,h) Intestinal Basal Lamina Thickness (μm), d,i) Intestinal Muscle Thickness (μm) and e,j) Number of intestinal goblet cells counted in 100 μm of fold length in female and male gut respectively, in the different experimental groups. Data are reported as mean ± standard deviation (SD) ($n = 6$). Letter "a" has been assigned to the highest value. Groups with the same letters do not present statistically significant differences among them, whereas groups with different letters do present statistically significant differences among them ($P < 0.05$). Groups labeled with two letters do not present statistically significant differences with other groups presenting either of them. Microphotographs show representative hematoxylin and eosin and alcian blue stainings in the different experimental groups. Scale bar = 50 μm.

3.2. Histopathological analysis of liver and brain

The histopathological analysis of the liver revealed that the exposure to BPA triggered vacuolar degeneration (female = +; male = +++) and sinusoid dilation (female = ++; male = +++), especially in the males, and a depletion of glycogen in both sexes (female = +++; male = +++). The percentage of the fish showing such hepatic alterations was lower in the BPA-exposed fish co-treated with the probiotic (female = +, −, −; male = +, +, + respectively) (Table 1). Concerning liver apoptosis, the percentage of TUNEL-positive areas was significantly higher in the fish exposed to BPA but decrease down to the C and P levels in the BPA-exposed females co-treated with SLAB51, whereas in BPA-exposed males the apoptotic levels were reduced when SLAB51 was administered but they still remain higher than in the C and P groups (Fig. 2 a,b). Likewise, the histopathological analysis in the brain showed that BPA exposure, especially in males, increased the neuronal degeneration (female = +; male = ++), micro vessel alterations (female = ++; male = +++), and perivascular edema (female = ++; male = +++). The percentage of the fish showing such brain alterations was lower in the BPA-exposed fish co-treated with the probiotic (female = −, +, −; male = +, ++, ++, respectively) (Table 2). Besides, the TUNEL assay in the brain sections showed a higher percentage of apoptotic areas in the BPA-exposed fish, being this percentage significantly reduced by the probiotic co-treatment in male while co-treated female showed absence of this damage (Fig. 3 a,b). The neurological toxicity of BPA and the mitigating capacity of the probiotic were supported by the quantification of GFAP, secreted by astrocytes after brain injury, and the TAU aggregates, associated with neuronal damage. The immunohistochemistry assay showed that both of them were significantly higher in the BPA-exposed fish, mainly in the male brains, whereas such levels were reduced, down to C and P levels in the case of females, when SLAB51 was co-administered (Fig. 3 c-f).

3.3. Burst respiratory assay

The oxidative burst is used as endpoint study in teleost to measure the release of reactive oxygen species (ROS), predominantly from neutrophils, as a defense mechanism against different pathogens (Hampton

Table 1
Liver histopathology. Histopathological score assigned to each sample in each group for vacuolar degeneration, sinusoid dilation, and glycogen depletion in female and male, from different experimental groups (n = 3 for all groups both in female and male).

	C			BPA			BPA + P			P		
Female												
Vacuolar degeneration	−	−	+	+	+	++	−	+	+	−	−	−
Sinusoid dilation	−	−	−	++	++	+++	−	−	+	−	−	−
Glycogen depletion	−	−	+	++	+++	+++	−	−	+	−	−	−
Male												
Vacuolar degeneration	−	−	+	+++	+++	+++	+	+	++	−	−	−
Sinusoid dilation	−	−	−	+++	+++	+++	+	+	++	−	−	−
Glycogen depletion	−	−	+	++	+++	+++	+	+	++	−	−	+

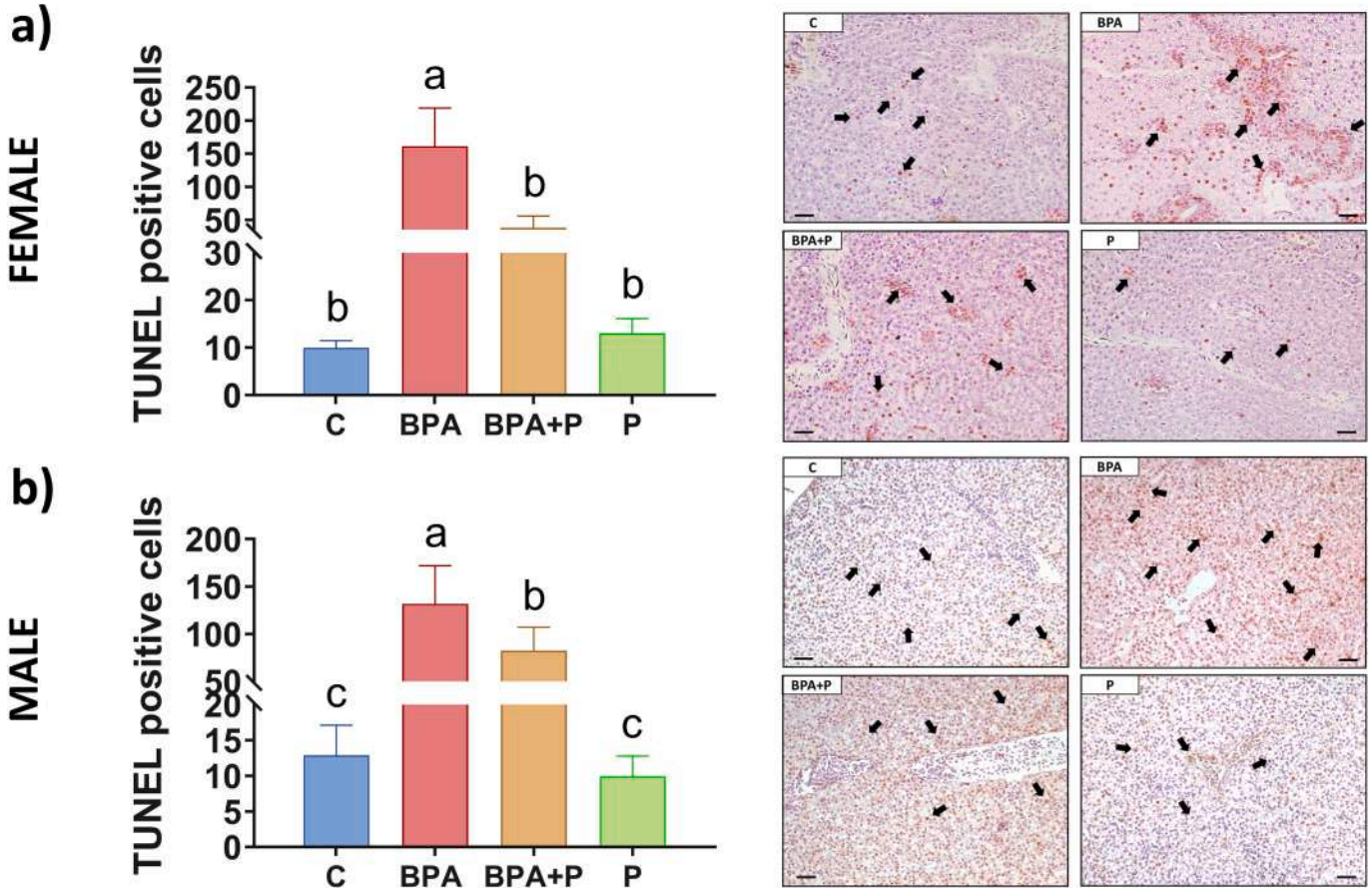

Fig. 2. Liver TUNEL. TUNEL positive cells in a) female and b) male liver in the experimental groups. Data are reported as mean ± standard deviation (SD) ($n = 3$). Groups with the same letters do not present statistically significant differences among them, whereas groups with different letters do present statistically significant differences among them ($P < 0.05$). Letter "a" has been assigned to the highest value. Microphotographs show representative images of TUNEL assay in the female (upper) and male (lower) liver sections in which the TUNEL positive cells are indicated by black arrows. Scale bar = 200 μm.

et al., 2020). The results showed that, in both sexes (Fig. 4 a,b), the burst respiratory was similar in C and P groups, but the differences before and after the stimulation with phorbol 12-myristate 13-acetate (PMA) were more remarkable in the group treated with the probiotic mixture. In female fish, the exposure to BPA led to a reduction of ROS production before and after stimulation when compared to the other experimental groups. Interestingly, it was the only group in which this response did not increase after stimulation with PMA. The probiotic co-treatment slightly increased the sensitivity of lymphocytes before and after stimulation, although remained still significantly lower when compared to both C and P groups. In males, the exposure to BPA significantly reduced the burst activity but, differently from the results obtained in females, the stimulation with PMA increased the baseline response that was initially lower. Similarly, when BPA-exposed fish were co-treated with SLAB51, this response was significantly increased both before and after stimulation, but still remains lower than the burst activities observed in the C and P groups.

3.4. Assessment of metabolomic phenotypes

The application of MAVEN software associated with a standard library allowed the identification of 43 metabolites in the liver extracts. PCA was conducted on metabolic data obtained from all male and female and the QC groups. The PCA scatter plot showed a strong cluster formation for the QC group (Supplementary Fig. 3) and did not discriminate among the other experimental groups. Thus, PLS-DA analysis was performed in both females (Supplementary Fig. 4) and males (Supplementary Fig. 5) by combining dimensionality reduction and discriminant analysis to further investigate separation among groups. In females, PLS-DA analysis revealed a partial overlap between C and BPA-exposed fish and between P and BPA + P groups (Supplementary Fig. 4 a). In males, the PLS-DA analysis showed a different metabolic profile for C, BPA, and P groups, while the metabolomic profile of BPA + P group partially overlapped with both BPA and P groups (Supplementary Fig. 5 a). The further analysis in a pair-wise manner demonstrated a clear separation between C and the other experimental groups in both sexes (Supplementary Fig. 4 b-f and 5 b-f, respectively). VIP > 1 were selected based on PLS-DA projections and are reported in Supplementary Table 3 and 4.

Volcano plots were used to display significant VIP > 1 changes [−log10 (*p*-value) and log2(FC)] comparing C with all other experimental groups in female (Fig. 5 a,c,e) and male (Fig. 5 b,d,f) zebrafish and comparing BPA + P with BPA and P in females and males (Supplementary Fig. 6). Interestingly, in females, BPA exposure led to a significant increase in Fructose 1,6-bis phosphate (FBP), Docosahexaenoic acid (DHA), Uridine diphosphate glucose (UDP glucose), Acetoacetic acid (AcAC), Dihydroxyacetone phosphate (DHAP) and O-Phosphoethanolamine (PE) when compared to C group (Fig. 5 a). AcAC and UDP glucose were also increased, together with β-Alanyl-3-methylhistidine (Anserine) in BPA-exposed females co-treated with SLAB51, whereas lower levels of Retinoic acid (RA) were found in these samples (Fig. 5 c). The administration of SLAB51 significantly increased the Anserine levels but decreased those of *N*-methyl-L-glutamic acid (methylglutamate) (Fig. 5 e). In the case of male livers few metabolites changed when compared to the C group, but some of them are still noteworthy: Glutathione (GSH) levels were significantly increased after

Table 2
Brain histopathology. Histopathological score assigned to each sample in each group for neuronal degeneration, microvessel alteration and perivascular edema in female and male in different experimental groups (n = 6 for C and BPA in both sexes and for BPA + P and P male, n = 4 for P female and n = 8 for BPA + P female).

Female	C						BPA						BPA + P						P					
Neuronal Degeneration	−	−	−	−	−	+	−	−	++	+	+	−	−	+	+	−	−	−	−	−	−	−	−	−
Microvessels Alterations	−	−	−	−	−	++	++	++	+	++	+	+	−	+	+	−	−	+	−	−	−	−	−	−
Perivascular Edema	+	−	−	+	+	++	+	++	−	++	+	−	−	−	+	+	−	−	+	−	−	−	+	−

Male	C						BPA						BPA + P						P					
Neuronal Degeneration	−	−	−	−	−	++	+	++	++	++	++	+	+	++	−	+	−	+	+	−	−	−	−	−
Microvessels Alterations	−	+	−	+	−	++	++	++	++	++	++	++	++	++	+	++	+	++	−	+	−	+	+	−
Perivascular Edema	+	−	++	+	−	++	++	++	++	++	++	+	++	++	+	+	++	+	+	−	+	−	+	−

BPA exposure (Fig. 5 b), whereas the co-treatment with SLAB51 increased the Anserine level and reduced those of Glutamine (Fig. 5 d). Dot plots show the impact of each metabolite within biological pathways. The pathways are detailed in Supplementary Table 5 and 6.

3.5. Metagenomic analysis of intestine samples

The analysis of gut bacterial composition among the different experimental groups showed differences in the phylum abundance. The alpha diversity revealed significant differences, in both sexes, between the C and the other experimental groups (Supplementary Table 7). Subsequently, a statistical analysis was conducted to assess changes at genus level using those that contributed at least 1 % of the total abundance. Based on these data, *Staphylococcus* showed a higher abundance in the females exposed to BPA when compared with the other experimental groups, whereas *Cetobacterium* was more abundant in the BPA-exposed males co-treated with SLAB51 when compared to both C and BPA-exposed groups (Fig. 6 b). In the males, both *Plesiomonas* and *Pirellula* were less abundant in the BPA-exposed group co-treated with SLAB51, when compared to the C group and to both BPA and P group, respectively (Fig. 6 c).

A predictive analysis was conducted to analyze the pathways in which bacteria colonizing the gut in different treatments are involved and results are summarized in Fig. 6 d,e.

4. Discussion

In this study we employed a multidisciplinary approach that integrates histological, immunohistochemical, metabolomic, and metagenomic data. Our findings demonstrate the ability of SLAB51 to counteract BPA toxicity in zebrafish, thereby restoring the homeostasis of the gut microbiota-liver-brain axis.

Even though the capacity of BPA and other plasticizers to induce intestinal inflammation and damage has been largely described *in vivo* and *in vitro*, in mammalian models (Liu et al., 2022; Ni et al., 2021; Wang et al., 2021), little is known regarding fish. Only few studies have reported that BPA exposure increases the oxidative stress in the gut (Elizalde-Velázquez et al., 2023) and alters microbiome composition (Adamovsky et al., 2021; Catron et al., 2019). The histopathological results herein reported strongly confirmed the intestinal BPA toxicity in both male and female zebrafish, showing similar damages to those observed in teleost exposed to heavy metals (Abdelazim et al., 2018; Hoseini et al., 2022; Wang et al., 2023). SLAB51, when co-administered with BPA, was able to recover the gut architecture comparable to that of control group, thus confirming the beneficial capacity of this probiotic mixture to mitigate the EDC toxicity. This is in accordance with previous studies in which the administration of *L. plantarum* ST-III reduced the intestinal inflammation caused by Triclosan (Zang et al., 2019) and *L. rhamnosus* GG increased the intestinal mucous production displaying protective effects against PFBS toxicity (Hu et al., 2021). Likewise, when SLAB51 was co-administered to BPA-exposed males, it increased the number of goblet cells, which produce acid mucins, thus enhancing the epithelial protection.

Goblets cells, together with the enterocytes, enteroendocrine cells, neurons, and glial cells in the CNS conformed the gut-brain axis, whose study has established the association of gastrointestinal distress with different neurological disorders (James et al., 2021). Therefore, a histopathological analysis of both male and female brains was conducted in all the experimental groups. The results revealed that males are particularly vulnerable to BPA exposure, exhibiting high levels of neurological degeneration, micro-vessel alterations, and perivascular edema. These results agree with previous observations in mice exposed to different bisphenols (including BPA) showing that males are more prone to neurotoxicity than female specimens (Meng et al., 2021). In addition, several studies evidenced the capacity of BPA to induce apoptosis: exposure to 10^{-4} M (22.8 μg/L) BPA for 5 days increased the percentage

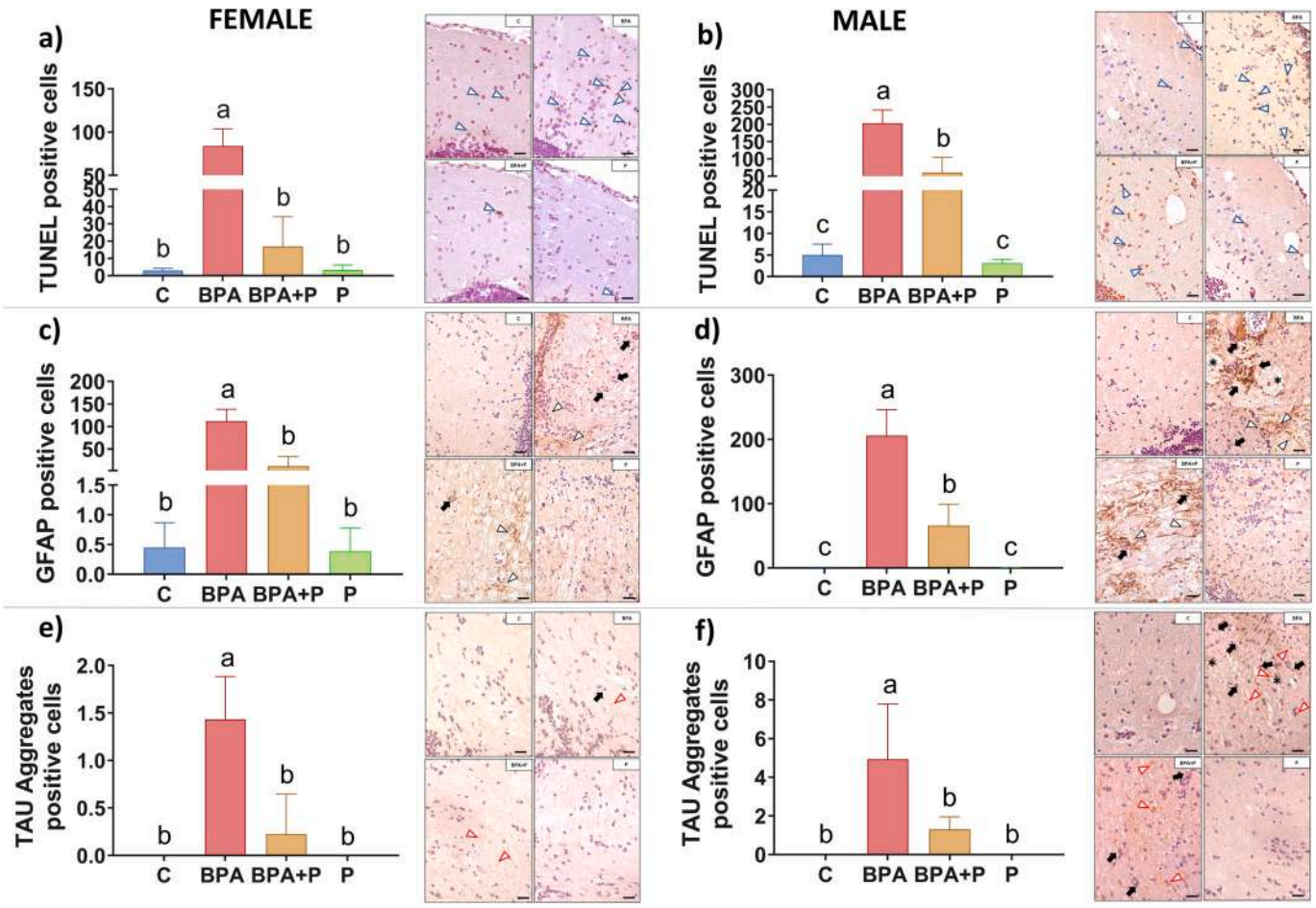

Fig. 3. Brain TUNEL and IHC. a,b) TUNEL, c,d) GFAP and e,f) TAU aggregates positive cells of female and male brains respectively, in different experimental groups. Data are reported as mean ± standard deviation (SD). Groups with the same letters do not present statistically significant differences among them, whereas groups with different letters do present statistically significant differences among them ($P < 0.05$) ($n = 6$ for C and BPA in both sexes and for BPA + P and P male, $n = 4$ for P female and $n = 8$ for BPA + P female). Letter "a" has been assigned to the highest value. Microphotographs show representative images of TUNEL, GFAP and TAU in the female (left) and male (right) brain sections. Scale bar = 200 μm.

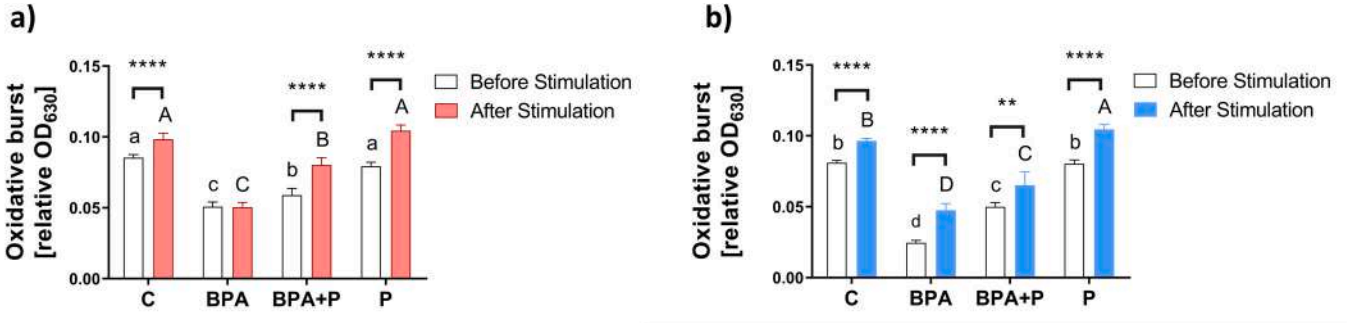

Fig. 4. Respiratory Burst Assay. Spleen respiratory burst assay in the different experimental groups before (white) and after stimulation with PMA [red in female (a) and blue in male (b)]. Data are reported as mean ± standard deviation (SD). Asterisks indicate statistically significant differences before and after PMA stimulation (**$P < 0.01$, ****$P < 0.0001$), whereas lower-case letters indicate statistically significant differences among the groups before stimulation and upper-case letters after the stimulation ($n = 6$, $P < 0.05$). Letter "a" and "A" has been assigned to the highest value.

of rat embryonic midbrain apoptotic cells (Liu et al., 2013), whereas exposure to 1 and 4 mg/L BPA for 56 days increased the levels of cleaved-caspase 3 of both zebrafish diencephalon and the telencephalon (Sahoo et al., 2021). Moreover, this toxicant has been reported to promote the formation of TAU aggregates (Elbakry et al., 2022), leading to the development and progression of tauopathies. In this context, previous studies using a transgenic mouse model of Alzheimer (Bonfili et al., 2022b, 2022a) and Parkinson's disease (Castelli et al., 2021) showed that SLAB51 administration, by modulating the host microflora, significantly ameliorated these neurological tauopathies. In addition, in zebrafish, the administration of *L. rhamnosus* reduced the neurotoxicity induced by PFBS (Liu et al., 2020). Noteworthy, in the present study, the co-treatment of BPA with SLAB51, not only reduced the high levels of GFAP and TAU aggregates triggered by BPA exposure, but also

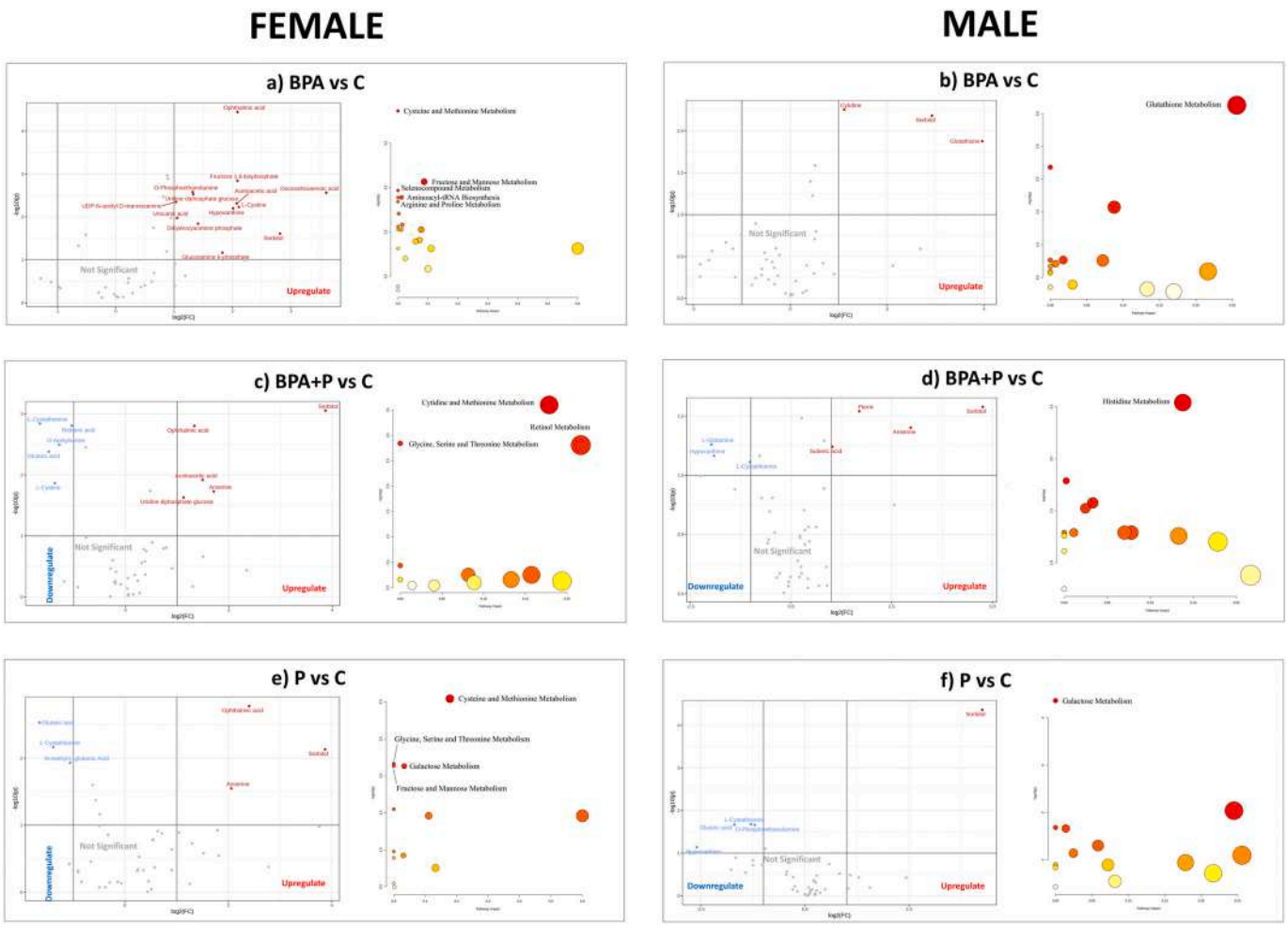

Fig. 5. Liver metabolomic analysis. Volcano plot and pathway analysis of BPA *vs* C, BPA + P *vs* C and P *vs* C in a,c,e) female and b,d,f) male ($n = 5$ for both C and BPA + P, $n = 6$ for both BPA and P in female, $n = 4$ for all groups in male). In volcano plot, up-regulated metabolites are shown in red, down-regulated metabolites are shown in blue and not-significant metabolites are shown in grey. The X axis stands for the relevance of the metabolite within the pathway, whereas the Y for the significance of the pathway in the comparison. The color of the dots represents the level of statistical significance, red being the most statistically significant and white the least. The width of the dots indicates the relevance of the metabolites inside that pathway, the wider they are, the greater relevance they have.

counteracted the histopathological damage and the high levels of apoptosis in both male and female fish. The concomitant reduction of the hepatic glutamine levels observed in BPA + P co-exposed males highlighted the beneficial action of probiotic administration. In normal physiological conditions, glutamine can be converted into glutamate and ammonia, which then exit the liver and reach the CNS. They cross the blood-brain barrier and trigger the release of proinflammatory factors that can compromise memory functions (Limón et al., 2021). Thus, probiotics seem to exert a protective role by regulating glutamine, aiding in the defense against neurological disorders (D'Mello and Swain, 2011). This protective role of the probiotics may be, to a certain extent, a result of the liver-brain communication pathway as well.

As for other liver metabolites, BPA exposure in females increased UDP-Glucose levels, which correlates with the glycogen depletion evidenced by histological analysis. This agrees with previous data on BPS exposure in zebrafish, showing that BPS is able to stimulate glycogenolysis (Zhao et al., 2018). This metabolite is produced in physiological conditions as an intermediate for glycogen synthesis (Adeva-Andany et al., 2016) and is directly linked to DHAP, which is increased when glucose levels rise. Consistent with the evidence of glycogen shortage and impaired glycolysis and gluconeogenesis, the metabolomic analysis showed a hepatic rise of AcAc, one of the three main ketone bodies. This metabolite is frequently associated with the onset of ketoacidosis state, a disorder characterized by increased mobilization of free fatty acids from lipid stores and excessive conversion within the hepatocytes into ketone bodies. Ketogenesis occurs in fasting conditions and is generally associated with increased oxidative stress (Kanikarla-Marie and Jain, 2016; Shi et al., 2016). Thus, the alterations of glucose metabolism in BPA-exposed females could be linked to a fasting state scenario where fatty acids are catabolized to form ketone bodies for energy production. AcAc is an indispensable source of energy for extrahepatic tissues and a source of cholesterol, fatty acids, and complex lipids (Ghimire and Dhamoon, 2023). In this context, the increased levels of DHA, an omega-3 fatty acid, can be used as an energy source for lipogenesis or can bind to nuclear hormone receptors, promoting the transcription of genes involved in adipogenesis and lipogenesis (Hardwick et al., 2009). Moreover, the increase in PE, an ethanolamine derivative used as a source of phospholipids (Hayase et al., 1986) suggests a higher energy demand since these lipids were not retained in the liver, as indicated by the absence of steatosis in BPA-exposed females, as already reported by other studies in zebrafish using the same dose (Forner-Piquer et al., 2018), reinforcing the idea that female specimens are more tolerant to BPA toxicity. On the contrary, in males the widely described ability of BPA to induce hepatic steatosis (Sun et al., 2019; Tian et al., 2021) was herein confirmed as a result of the higher vacuolar degeneration, fibrosis cell ballooning, and sinusoid dilation, clear signs that herald the onset of fatty liver disease. Eventually this glycogen depletion could be linked to its excessive use in the "starch biosynthesis" pathway in BPA-exposed

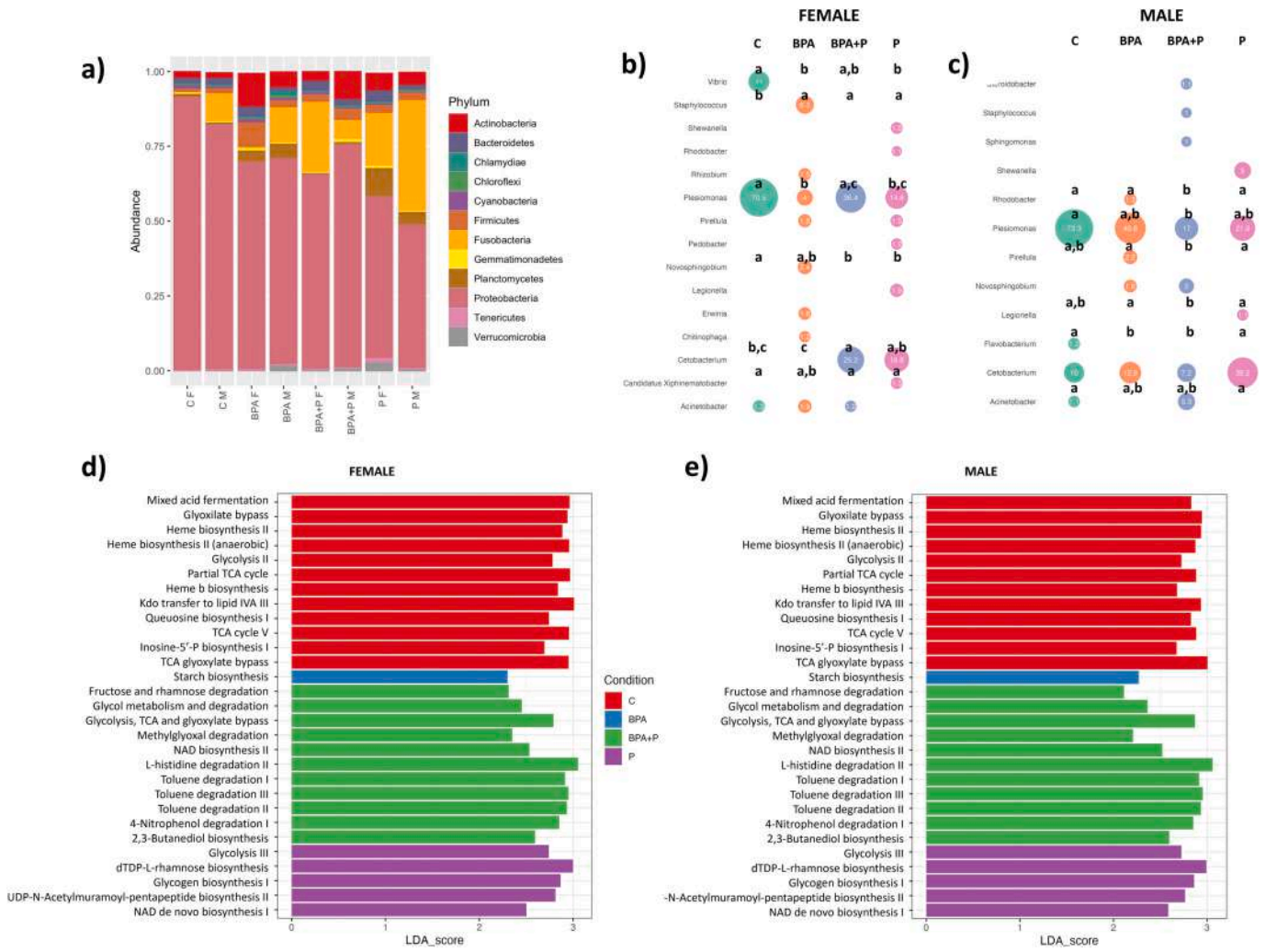

Fig. 6. Microbiota analysis. a) Stacked bar chart representing the relative abundance of bacterial phyla in both sexes (only taxa contributing to at least 1 % of the total composition are displayed). Bubble chart showing genera abundance analysis in different groups (abundance >1 % of the total composition are displayed), determined by DESeq2 and adjusted for multiple comparisons (Benjamini-Hochberg) for b) females and c) males respectively (n = 6 for C both females and males and n = 3 for BPA, BPA + P and P for both females and males). Bubble size indicates higher (big) or lower (small) absolute abundance of bacterial genera. Letter "a" has been assigned to the highest value. Groups with the same letters do not present statistically significant differences among them, whereas groups with different letters do present statistically significant differences among them ($P < 0.05$). Groups labeled with two letters do not present statistically significant differences with other groups presenting either of them. LEFSa pathway prediction analysis based on gut microbial colonization data of d) females and e) males.

fish, as revealed by the prediction analysis. Through this pathway, Cyanobacteria produce starch from glucose as energy source (Ball et al., 2015). Noteworthy, SLAB51 reduced the BPA-induced glycogen depletion in the co-treated group, being only AcAc and UDP-Glucose still increased. Interestingly, the BPA-induced glycogen depletion has been recently linked to neurotoxicity through the alterations of intrahepatic parasympathetic nerves in juvenile porcine (Thoene et al., 2017). This evidence could explain the results we observed regarding BPA-induced damage found at liver and brain levels and suggests the possibility that the mitigation of glycogen depletion, operated by SLAB51 at peripheral level, could also contribute to mitigate neurotoxicity. Furthermore, in males exposed to BPA, the rise of GSH levels suggests its accumulation instead of its use as antioxidant substrate (Bonfili et al., 2018), well supporting the low levels of ROS production in the spleen. By contrast, when SLAB51 was administered to BPA-exposed fish, favored the increase of anserine, which could contrast GSH accumulation. In fact, anserine has been reported to enhance glutathione disulfide (GSSG) and, consequently, lowered the glutathione-to-glutathione disulfide (GSH/GSSG) ratio (Alkhatib et al., 2020). Therefore, its increase when co-treating the BPA-exposed fish with probiotic could mitigate the imbalance of GSH/ROS that could also affect the immune response. Moreover, anserine suppresses glial neuroinflammatory reaction in a mice Alzheimer's model (Kaneko et al., 2017), thus its increased levels found in both females and males exposed to BPA and co-treated with the probiotic could once again contribute to the reduction of GFAP caused by BPA exposure.

Even though the species contained in the SLAB51 mixture do not colonize the gut of the host, as already demonstrated for other probiotics (Gioacchini et al., 2018), it is able to favor the colonization of other bacteria, as shown by the results, and in turn to shape the host microbiota. For example, in BPA + P exposed male, the probiotic co-administration decreased colonization of *Plesiomonas,* a pathogenic bacterium causing enteritis and diarrhea in human and freshwater fish (Behera et al., 2018), and *Pirellula*, a bacteria presenting different antibiotic resistance (Clum et al., 2009). Moreover, SLAB51 was also able to control the BPA-induced changes of *Staphyloccocus* abundance. It has been reported that zebrafish embryos infected with *Staphyloccocus aureus* showed a reduced burst respiratory, but when they were co-treated with epigallocatechin gallate (Stevens et al., 2015), a mitigating substance from green tea, the burst respiratory was increased.

Herein we have observed an absence of changes before and after PMA stimulation in females treated with BPA that could be also linked to the higher abundance of *Staphyloccocus* found in the gut of these females. Interestingly, when we co-administered the probiotic, the burst respiratory levels were restored and the abundance of *Staphyloccocus* was reduced. All these aspects could cooperate to improve the fish immune response, strongly suggesting the beneficial effect of this probiotic administration against BPA injuries. Interestingly, SLAB51 administration, both alone or in combination with BPA and in both sexes, enhanced the colonization of bacteria in charge of *de novo* NAD biosynthesis. Different bacteria are able to catabolize BPA through diverse reactions that depend on NAD as coenzyme (Chouhan et al., 2014). This evidence, together with the pathways involved in the catabolism of organic xenobiotic compounds in BPA + P group, suggests that the probiotic administration enhances BPA catabolism, consequently reducing its toxicity as observed in BPA + P fish. Furthermore, BPA catabolism is a retinol-dependent process, as demonstrated by Shmarakov et al. (2017) who observed an absence of BPA detoxification in mice lacking hepatic retinoid stores (*Lrat*$^{-/-}$) when compared to wild-type mice, being this deficient mechanism rescued after retinyl acetate administration. The retinoid that is not stored in the liver is metabolized oxidatively, resulting in retinaldehyde and retinoic acid. Hence, the reduction of retinoic acid in the livers of BPA-exposed females co-treated with the probiotic could result from the increased storage of retinoid in the liver of these female, reinforcing the fact that SLAB51 enhances the pollutant elimination.

5. Conclusions

This is the first study in which the deleterious effects of BPA on gut microbiota-liver-brain axis have been demonstrated in zebrafish since the toxicity of this compound had been so far studied in single organs. Altogether, the results confirmed the hypothesis that SLAB51 is able to counteract the pleiotropic toxicity of BPA by modulating gut microbiota and mitigating the alterations in gut architecture and the histopathological damage at both liver and brain levels. Moreover, in this study we have provided evidence of how probiotics can modulate gut microbiota and liver metabolism, thus maintaining not only the intestinal and hepatic homeostasis but also brain function. However, a bidirectional crosstalk among these organs should be considered before implementing the probiotics as a possible therapy to counteract EDC toxicity since the enteric, hepatic, and nervous systems are connected by a complex multidirectional communication network.

Funding

This work was supported by Fondi di Ateneo, Università Politecnica delle Marche to O.C. and by the funding from Natural Sciences and Engineering Research Council of Canada to H.R.H. (NSERC Discovery Grant; project no. 1254045). M.L. is supported by a postdoctoral contract (Ayudas Margarita Salas para la formación de jóvenes doctores, convocatoria de la Universidad de León de Ayudas para la recualificación del sistema Universitario español para 2021–2023). CL was in part supported by the Alberta Graduate Excellence Scholarship (AGES) and NSERC grant to H.R.H.

CRediT authorship contribution statement

Christian Giommi: Data curation, Formal analysis, Methodology, Software, Validation, Writing – original draft. **Marta Lombo:** Data curation, Validation, Writing – original draft. **Hamid R. Habibi:** Conceptualization, Funding acquisition, Methodology, Writing – review & editing. **Giacomo Rossi:** Conceptualization, Data curation, Formal analysis, Funding acquisition, Methodology, Validation, Writing – original draft. **Danilo Basili:** Methodology, Software, Validation. **Sara Mangiaterra:** Formal analysis. **Claudia Ladisa:** Formal analysis, Methodology. **Giulia Chemello:** Data curation. **Oliana Carnevali:** Funding acquisition, Writing – review & editing, Supervision. **Francesca Maradonna:** Conceptualization, Methodology, Writing – original draft.

Declaration of competing interest

The authors declare no competing interests.

Data availability

Data will be made available on request.

Acknowledgements

The Authors wish to thank Dr. Matteo Zarantoniello for kindly providing the picture of zebrafish for the graphical abstract.

Appendix A. Supplementary data

Supplementary data to this article can be found online at https://doi.org/10.1016/j.scitotenv.2023.169303.

References

Abdelazim, A.M., Saadeldin, I.M., Swelum, A.A.A., Afifi, M.M., Alkaladi, A., 2018. Oxidative stress in the muscles of the fish Nile tilapia caused by zinc oxide nanoparticles and its modulation by vitamins C and E. Oxidative Med. Cell. Longev., 6926712 https://doi.org/10.1155/2018/6926712.

Adamovsky, O., Bisesi, J.H., Martyniuk, C.J., 2021. Plastics in our water: fish microbiomes at risk? Comp. Biochem. Physiol. Part D. Genom. Proteom. 39, 100834 https://doi.org/10.1016/J.CBD.2021.100834.

Adeva-Andany, M.M., Pérez-Felpete, N., Fernández-Fernández, C., Donapetry-García, C., Pazos-García, C., 2016. Liver glucose metabolism in humans. Biosci. Rep. 36 (6), 416. https://doi.org/10.1042/BSR20160385.

Alkhatib, A., Feng, W.-H., Huang, Y.-J., Kuo, C.-H., Hou, C.-W., 2020. Anserine reverses exercise-induced oxidative stress and preserves cellular homeostasis in healthy men. Nutrients 12 (4), 1146. https://doi.org/10.3390/NU12041146.

Ball, S., Colleoni, C., Arias, M.C., 2015. In: Nakamura, Y. (Ed.), The Transition from Glycogen to Starch Metabolism in Cyanobacteria and Eukaryotes. Springer, Tokyo, pp. 93–158. https://doi.org/10.1007/978-4-431-55495-04.

Behera, B.K., Bera, A.K., Paria, P., Das, A., Parida, P.K., Kumari, S., Bhowmick, S., Das, B. K., 2018. Identification and pathogenicity of Plesiomonas shigelloides in silver carp. Aquaculture 493, 314–318. https://doi.org/10.1016/J.AQUACULTURE.2018.04.063.

Beule, L., Karlovsky, P., 2020. Improved normalization of species count data in ecology by scaling with ranked subsampling (SRS): application to microbial communities. PeerJ 8, e9593. https://doi.org/10.7717/peerj.9593.

Bonfili, L., Cecarini, V., Cuccioloni, M., Angeletti, M., Berardi, S., Scarpona, S., Rossi, G., Eleuteri, A.M., 2018. SLAB51 probiotic formulation activates SIRT1 pathway promoting antioxidant and neuroprotective effects in an AD mouse model. Mol. Neurobiol. 55 (10), 7987–8000. https://doi.org/10.1007/S12035-018-0973-4.

Bonfili, L., Cuccioloni, M., Gong, C., Cecarini, V., Spina, M., Zheng, Y., Angeletti, M., Eleuteri, A.M., 2022a. Gut microbiota modulation in Alzheimer's disease: focus on lipid metabolism. Clin. Nutr. 41, 698–708. https://doi.org/10.1016/j.clnu.2022.01.025.

Bonfili, L., Gong, C., Lombardi, F., Cifone, M.G., Eleuteri, A.M., 2022b. Strategic modification of gut microbiota through Oral Bacteriotherapy influences hypoxia inducible factor-1α: therapeutic implication in Alzheimer's disease. Int. J. Mol. Sci. 23 https://doi.org/10.3390/IJMS23010357.

Bordbar, H., Yahyavi, S.S., Noorafshan, A., Aliabadi, E., Naseh, M., 2023. Resveratrol ameliorates bisphenol A-induced testicular toxicity in adult male rats: a stereological and functional study. Basic Clin. Androl. 33 (1), 1. https://doi.org/10.1186/S12610-022-00174-8.

Caicedo, H.H., Hashimoto, D.A., Caicedo, J.C., Pentland, A., Pisano, G.P., 2020. Overcoming barriers to early disease intervention. Nat. Biotechnol. 38, 669–673. https://doi.org/10.1038/s41587-020-0550-z.

Castelli, V., d'Angelol, M., Lombardi, F., Alfonsetti, M., Antonosante, A., Catanesi, M., Benedetti, E., Palumbo, P., Cifone, M.G., Giordano, A., Desideri, G., Cimini, A., 2020. Effects of the probiotic formulation SLAB51 in in vitro and in vivo Parkinson's disease models. Aging 12 (5), 4641–4659. https://doi.org/10.18632/AGING.102927.

Castelli, V., D'Angelo, M., Quintiliani, M., Benedetti, E., Cifone, M.G., Cimini, A., 2021. The emerging role of probiotics in neurodegenerative diseases: new hope for Parkinson's disease? Neural Regen. Res. 16 (4), 628–634. https://doi.org/10.4103/1673-5374.295270.

Catron, T.R., Keely, S.P., Brinkman, N.E., Zurlinden, T.J., Wood, C.E., Wright, J.R., Phelps, D., Wheaton, E., Kvasnicka, A., Gaballah, S., Lamendella, R., Tal, T., 2019.

Host developmental toxicity of BPA and BPA alternatives is inversely related to microbiota disruption in zebrafish. Toxicol. Sci. 167 (2), 468–483. https://doi.org/10.1093/toxsci/kfy261.

Chen, L., Guo, Y., Hu, C., Lam, P.K.S., Lam, J.C.W., Zhou, B., 2018. Dysbiosis of gut microbiota by chronic coexposure to titanium dioxide nanoparticles and bisphenol a: implications for host health in zebrafish. Environ. Pollut. 234, 307–317. https://doi.org/10.1016/J.ENVPOL.2017.11.074.

Chen, L., Lam, J.C.W., Tang, L., Tang, L., Hu, C., Liu, M., Liu, M., Lam, P.K.S., Zhou, B., 2020. Probiotic modulation of lipid metabolism disorders caused by Perfluorobutanesulfonate pollution in zebrafish. Environ. Sci. Technol. 54 (12), 7494–7503. https://doi.org/10.1021/ACS.EST.0C02345.

Chouhan, S., Yadav, S.K., Prakash, J., Swati, Singh, S.P., 2014. Effect of bisphenol a on human health and its degradation by microorganisms: a review. Ann. Microbiol. 64, 13–21. https://doi.org/10.1007/S13213-013-0649-2.

Clum, A., Tindall, B.J., Sikorski, J., Ivanova, N., Mavrommatis, K., Lucas, S., del Rio, T. G., Nolan, M., Chen, F., Tice, H., Pitluck, S., Cheng, J.F., Chertkov, O., Brettin, T., Han, C., Detter, J.C., Kuske, C., Bruce, A., Goodwin, L., Ovchinikova, G., Pati, A., Mikhailova, N., Chen, A., Palaniappan, K., Land, M., Hauser, L., Chang, Y.J., Jeffries, C.D., Chain, P., Rohde, M., Göker, M., Bristow, J., Eisen, J.A., Markowitz, V., Hugenholtz, H., Kyrpides, N.C., Klenk, H.P., Lapidus, A., 2009. Complete genome sequence of Pirellula staleyi type strain (ATCC 27377 T). Stand. Genomic Sci. 1, 308–316. https://doi.org/10.4056/sigs.51657.

Cryan, J.F., O'riordan, K.J., Cowan, C.S.M., Sandhu, K.V., Bastiaanssen, T.F.S., Boehme, M., Codagnone, M.G., Cussotto, S., Fulling, C., Golubeva, A.V., Guzzetta, K. E., Jaggar, M., Long-Smith, C.M., Lyte, J.M., Martin, J.A., Molinero-Perez, A., Moloney, G., Morelli, E., Morillas, E., O'connor, R., Cruz-Pereira, J.S., Peterson, V.L., Rea, K., Ritz, N.L., Sherwin, E., Spichak, S., Teichman, E.M., van de Wouw, M., Ventura-Silva, A.P., Wallace-Fitzsimons, S.E., Hyland, N., Clarke, G., Dinan, T.G., 2019. The microbiota-gut-brain Axis. Physiol. Rev. 99, 1877–2013. https://doi.org/10.1152/PHYSREV.00018.2018.

Cuozzo, M., Castelli, V., Avagliano, C., Cimini, A., D'angelo, M., Cristiano, C., Russo, R., 2021. Effects of chronic oral probiotic treatment in paclitaxel-induced neuropathic pain. Biomedicines 9 (4), 346. https://doi.org/10.3390/biomedicines9040346.

Dahiya, D., Nigam, P.S., 2022. Probiotics, prebiotics, synbiotics, and fermented foods as potential biotics in nutrition improving health via microbiome-gut-brain axis. Ferment 8 (7), 303. https://doi.org/10.3390/FERMENTATION8070303.

Desantis, S., Mastrodonato, M., Accogli, G., Rossi, G., Crovace, A.M., 2019. Effects of a probiotic on the morphology and mucin composition of pig intestine. Histol. Histopathol. 34 (9), 1037–1050. https://doi.org/10.14670/HH-18-106.

D'Mello, C., Swain, M.G., 2011. Liver-brain inflammation axis. Am. J. Physiol. Gastrointest. Liver Physiol. 301 (5), 749–761. https://doi.org/10.1152/AJPGI.00184.2011.

Elbakry, M.M.M., Mansour, S.Z., Helal, H., Ahmed, E.S.A., 2022. Nattokinase attenuates bisphenol a or gamma irradiation-mediated hepatic and neural toxicity by activation of Nrf2 and suppression of inflammatory mediators in rats. Environ. Sci. Pollut. Res. Int. 29 (49), 75086–75100. https://doi.org/10.1007/S11356-022-21126-9.

Elizalde-Velázquez, G.A., Gómez-Oliván, L.M., Herrera-Vázquez, S.E., Rosales-Pérez, K. E., SanJuan-Reyes, N., García-Medina, S., Galar-Martínez, M., 2023. Acute exposure to realistic concentrations of bisphenol-a trigger health damage in fish: blood parameters, gene expression, oxidative stress. Aquat. Toxicol. 261, 106610 https://doi.org/10.1016/J.AQUATOX.2023.106610.

European Food Safety Authority, 2023. Bisphenol A | EFSA. https://www.efsa.europa.eu/en/topics/topic/bisphenol. (Accessed 3 December 2023).

Feng, D., Zhang, H., Jiang, X., Zou, J., Li, Q., Mai, H., Su, D., Ling, W., Feng, X., 2020. Bisphenol a exposure induces gut microbiota dysbiosis and consequent activation of gut-liver axis leading to hepatic steatosis in CD-1 mice. Environ. Pollut. 265, 114880 https://doi.org/10.1016/J.ENVPOL.2020.114880.

Forner-Piquer, I., Santangeli, S., Maradonna, F., Verde, R., Piscitelli, F., di Marzo, V., Habibi, H.R., Carnevali, O., 2018. Role of bisphenol a on the endocannabinoid system at central and peripheral levels: effects on adult female zebrafish. Chemosphere 205, 118–125. https://doi.org/10.1016/j.chemosphere.2018.04.078.

Ghimire, P., Dhamoon, A.S., 2023. Ketoacidosis. In: StatPearls. StatPearls Publishing, Treasure Island (FL).

Gioacchini, G., Ciani, E., Pessina, A., Cinzia, C., Silvi, S., Rodiles, A., Merrifield, L.D., Olivotto, I., Carnevali, O., 2018. Effects of Lactogen 13, a new probiotic preparation, on gut microbiota and endocrine signals controlling growth and appetite of Oreochromis niloticus juveniles. Microb. Ecol. 76 (4), 1063–1074. https://doi.org/10.1007/S00248-018-1177-1.

Giommi, C., Habibi, H.R., Candelma, M., Carnevali, O., Maradonna, F., 2021. Probiotic administration mitigates bisphenol a reproductive toxicity in zebrafish. Int. J. Mol. Sci. 22 (17), 9314. https://doi.org/10.3390/ijms22179314.

Graham, S., Secombes, C.J., 1990. Cellular requirements for lymphokine secretion by rainbow trout Salmo gairdneri leucocytes. Dev. Comp. Immunol. 14, 59–68. https://doi.org/10.1016/0145-305X(90)90008-3.

Hampton, L.M.T., Jeffries, M.K.S., Venables, B.J., 2020. A practical guide for assessing respiratory burst and phagocytic cell activity in the fathead minnow, an emerging model for immunotoxicity. MethodsX 7, 100992. https://doi.org/10.1016/J.MEX.2020.100992.

Hardwick, J.P., Osei-Hyiaman, D., Wiland, H., Abdelmegeed, M.A., Song, B.J., 2009. PPAR/RXR regulation of fatty acid metabolism and fatty acid ω-hydroxylase (CYP4) isozymes: implications for prevention of lipotoxicity in fatty liver disease. PPAR Res. 2009, 952734 https://doi.org/10.1155/2009/952734.

Hayase, Y., Murakami, M., Takagi, Y., 1986. Determination of O-phosphoethanolamine in male and female mouse tissues by high-performance liquid chromatography. Yakugaku Zasshi 106 (8), 694–697. https://doi.org/10.1248/YAKUSHI1947.106.8_694.

Hoseini, S.M., Sinha, R., Fazel, A., Khosraviani, K., Hosseinpour Delavar, F., Arghideh, M., Sedaghat, M., Paolucci, M., Hoseinifar, S.H., Van Doan, H., 2022. Histopathological damage and stress- and immune-related genes' expression in the intestine of common carp, Cyprinus carpio exposed to copper and polyvinyl chloride microparticle. J. Exp. Zool. Part A Ecol. Integr. Physiol. 337 (2), 181–190. https://doi.org/10.1002/JEZ.2555.

Hu, C., Liu, M., Tang, L., Liu, H., Sun, B., Chen, L., 2021. Probiotic intervention mitigates the metabolic disturbances of perfluorobutanesulfonate along the gut-liver axis of zebrafish. Chemosphere 284, 131374. https://doi.org/10.1016/j.chemosphere.2021.131374.

Jalili, V., Afgan, E., Gu, Q., Clements, D., Blankenberg, D., Goecks, J., Taylor, J., Nekrutenko, A., 2021. The Galaxy platform for accessible, reproducible and collaborative biomedical analyses: 2020. Nucleic Acids Res. 48, W395–W402. https://doi.org/10.1093/NAR/GKAA434.

James, D.M., Davidson, E.A., Yanes, J., Moshiree, B., Dallman, J.E., 2021. The gut-brain-microbiome Axis and its link to autism: emerging insights and the potential of zebrafish models. Front. Cell Dev. Biol. 9, 662916 https://doi.org/10.3389/FCELL.2021.662916.

Kaneko, J., Enya, A., Enomoto, K., Ding, Q., Hisatsune, T., 2017. Anserine (beta-alanyl-3-methyl-L-histidine) improves neurovascular-unit dysfunction and spatial memory in aged AβPPswe/PSEN1dE9 Alzheimer's-model mice. Sci. Report. 7 (1), 12571. https://doi.org/10.1038/s41598-017-12785-7.

Kanikarla-Marie, P., Jain, S.K., 2016. Hyperketonemia and ketosis increase the risk of complications in type 1 diabetes. Free Radic. Biol. 95, 268–277. https://doi.org/10.1016/j.freeradbiomed.2016.03.020.

Ladisa, C., Ma, Y., Habibi, H.R., 2021. Seasonally related metabolic changes and energy allocation associated with growth and reproductive phases in the liver of male goldfish (Carassius auratus). J. Proteome 241, 104237. https://doi.org/10.1016/j.jprot.2021.104237.

Lambré, C., Barat Baviera, J.M., Bolognesi, C., Chesson, A., Cocconcelli, P.S., Crebelli, R., Gott, D.M., Grob, K., Lampi, E., Mengelers, M., Mortensen, A., Rivière, G., Silano, V., Steffensen, I.L., Tlustos, C., Vernis, L., Zorn, H., Batke, M., Bignami, M., Corsini, E., FitzGerald, R., Gundert-Remy, U., Halldorsson, T., Hart, A., Ntzani, E., Scanziani, E., Schroeder, H., Ulbrich, B., Waalkens-Berendsen, D., Woelfle, D., Al Harraq, Z., Baert, K., Carfì, M., Castoldi, A.F., Croera, C., Van Loveren, H., 2023. Re-evaluation of the risks to public health related to the presence of bisphenol a (BPA) in foodstuffs. EFSA J. 21 (4), e06857 https://doi.org/10.2903/j.efsa.2023.6857.

Limón, I.D., Angulo-Cruz, I., Sánchez-Abdon, L., Patricio-Martínez, A., 2021. Disturbance of the glutamate-glutamine cycle, secondary to hepatic damage. Compromises memory function. Front. Neurosci. 15, 578922 https://doi.org/10.3389/FNINS.2021.578922.

Liu, M., Song, S., Hu, C., Tang, L., Lam, J.C.W., Lam, P.K.S., Chen, L., 2020. Dietary administration of probiotic Lactobacillus rhamnosus modulates the neurological toxicities of perfluorobutanesulfonate in zebrafish. Environ. Pollut. 265, 114832 https://doi.org/10.1016/j.envpol.2020.114832.

Liu, M., Tang, L., Hu, C., Huang, Z., Sun, B., Lam, J.C.W., Lam, P.K.S., Chen, L., 2021. Antagonistic interaction between perfluorobutanesulfonate and probiotic on lipid and glucose metabolisms in the liver of zebrafish. Aquat. Toxicol. 237, 105897 https://doi.org/10.1016/J.AQUATOX.2021.105897.

Liu, R., Cai, D., Li, X., Liu, B., Chen, J., Jiang, X., Li, H., Li, Z., Teerds, K., Sun, J., Bai, W., Jin, Y., 2022. Effects of bisphenol A on reproductive toxicity and gut microbiota dysbiosis in male rats. Ecotoxicol. Environ. Saf. 239, 113623 https://doi.org/10.1016/J.ECOENV.2022.113623.

Liu, R., Xing, L., Kong, D., Jiang, J., Shang, L., Hao, W., 2013. Bisphenol A inhibits proliferation and induces apoptosis in micromass cultures of rat embryonic midbrain cells through the JNK, CREB and p53 signaling pathways. Food Chem. Toxicol. 52, 76–82. https://doi.org/10.1016/J.FCT.2012.10.033.

Lombó, M., Herráez, M.P., 2021. Paternal inheritance of bisphenol a cardiotoxic effects: the implications of sperm epigenome. Int. J. Mol. Sci. 22 (4), 2–25. https://doi.org/10.3390/IJMS22042125.

Long-Smith, C., O'Riordan, K.J., Clarke, G., Stanton, C., Dinan, T.G., Cryan, J.F., 2020. Microbiota-gut-brain axis: new therapeutic opportunities. Annu. Rev. Pharmacol. Toxicol. 60, 477–502. https://doi.org/10.1146/ANNUREV-PHARMTOX-010919-023628.

Love, M.I., Huber, W., Anders, S., 2014. Moderated estimation of fold change and dispersion for RNA-seq data with DESeq2. Genome Biol. 15, 1–21. https://doi.org/10.1186/s13059-014-0550-8.

Ma, Y., Liu, H., Wu, J., Yuan, L., Wang, Y., Du, X., Wang, R., Marwa, P.W., Petlulu, P., Chen, X., Zhang, H., 2019. The adverse health effects of bisphenol A and related toxicity mechanisms. Environ. Res. 176, 108575 https://doi.org/10.1016/J.ENVRES.2019.108575.

Mangiaterra, S., Schmidt-Küntzel, A., Marker, L., Di Cerbo, A., Piccinini, R., Guadagnini, D., Turba, M.E., Berardi, S., Galosi, L., Preziuso, S., Cerquetella, M., Rossi, G., 2022. Effect of a probiotic mixture in captive cheetahs (Acinonyx Jubatus) with gastrointestinal symptoms—a pilot study. Animals 12 (3), 395, 12, 395. https://doi.org/10.3390/ANI12030395.

Manzoor, R., Ahmed, W., Afify, N., Memon, M., Yasin, M., Memon, H., Rustom, M., Al Akeel, M., Alhajri, N., 2022. Trust your gut: the Association of gut Microbiota and Liver Disease. Microorganisms 10 (5), 1045. https://doi.org/10.3390/MICROORGANISMS10051045.

Matsuzaki, R., Gunnigle, E., Geissen, V., Clarke, G., Nagpal, J., Cryan, J.F., 2023. Pesticide exposure and the microbiota-gut-brain axis. ISME J. 17, 1153–1166. https://doi.org/10.1038/S41396-023-01450-9.

McMurdie, P.J., Holmes, S., 2013. Phyloseq: an R package for reproducible interactive analysis and graphics of microbiome census data. PLoS One 8 (4), e61217. https://doi.org/10.1371/journal.pone.0061217.

Meng, L., Liu, J., Wang, C., Ouyang, Z., Kuang, J., Pang, Q., Fan, R., 2021. Sex-specific oxidative damage effects induced by BPA and its analogs on primary hippocampal neurons attenuated by EGCG. Chemosphere 264, 128450. https://doi.org/10.1016/J.CHEMOSPHERE.2020.128450.

Milosevic, I., Vujovic, A., Barac, A., Djelic, M., Korac, M., Spurnic, A.R., Gmizic, I., Stevanovic, O., Djordjevic, V., Lekic, N., Russo, E., Amedei, A., 2019. Gut-liver axis, gut microbiota, and its modulation in the management of liver diseases: a review of the literature. Int. J. Mol. Sci. 20 (2), 395. https://doi.org/10.3390/IJMS20020395.

Morais, L.H., Schreiber, H.L., Mazmanian, S.K., 2021. The gut microbiota-brain axis in behaviour and brain disorders. Nat. Rev. Microbiol. 19 (4), 241–255. https://doi.org/10.1038/S41579-020-00460-0.

Mu, X., Liu, Z., Zhao, X., Chen, L., Jia, Q., Wang, C., Li, T., Guo, Y., Qiu, J., Qian, Y., 2023. Bisphenol analogues induced social defects and neural impairment in zebrafish. Sci. Total Environ. 899, 166–307. https://doi.org/10.1016/J.SCITOTENV.2023.166307.

Ni, Y., Hu, L., Yang, S., Ni, L., Ma, L., Zhao, Y., Zheng, A., Jin, Y., Fu, Z., 2021. Bisphenol A impairs cognitive function and 5-HT metabolism in adult male mice by modulating the microbiota-gut-brain axis. Chemosphere 282, 130952. https://doi.org/10.1016/J.CHEMOSPHERE.2021.130952.

Oishi, K., Sato, T., Yokoi, W., Yoshida, Y., Ito, M., Sawada, H., 2008. Effect of probiotics, Bifidobacterium breve and Lactobacillus casei, on bisphenol a exposure in rats. Biosci. Biotechnol. Biochem. 72 (6), 1409–1415. https://doi.org/10.1271/bbb.70672.

Regulation (EU) 2016/1011 of the European Parliament and of the Council of 8 June 2016 on indices used as benchmarks in financial instruments and financial contracts or to measure the performance of investment funds and amending Directives 2008/48/EC and 2014/17/EU and Regulation (EU) No 596/2014.

Rossi, G., Pengo, G., Galosi, L., Berardi, S., Tambella, A.M., Attili, A.R., Gavazza, A., Cerquetella, M., Jergens, A.E., Guard, B.C., Lidbury, J.A., Stainer, J.M., Crovace, A. M., Suchodolski, J.S., 2020. Effects of the probiotic mixture Slab51® (SivoMixx®) as food supplement in healthy dogs: evaluation of fecal microbiota, clinical parameters and immune function. Front. Vet. Sci. 7, 613. https://doi.org/10.3389/FVETS.2020.00613.

Sahoo, P.K., Aparna, S., Naik, P.K., Singh, S.B., Das, S.K., 2021. Bisphenol A exposure induces neurobehavioral deficits and neurodegeneration through induction of oxidative stress and activated caspase-3 expression in zebrafish brain. J. Biochem. Mol. Toxicol. 35 (10), e22873 https://doi.org/10.1002/JBT.22873.

Segata, N., Izard, J., Waldron, L., Gevers, D., Miropolsky, L., Garrett, W.S., Huttenhower, C., 2011. Metagenomic biomarker discovery and explanation. Genome Biol. 12, R60. https://doi.org/10.1186/gb-2011-12-6-r60.

Shi, C., Han, X., Guo, W., Wu, Q., Yang, X., Wang, Y., Tang, G., Wang, S., Wang, Z., Liu, Y., Li, M., Lv, M., Guo, Y., Li, Z., Li, J., Shi, J., Qu, G., Jiang, G., 2022. Disturbed gut-liver axis indicating oral exposure to polystyrene microplastic potentially increases the risk of insulin resistance. Environ. Int. 164, 107273 https://doi.org/10.1016/J.ENVINT.2022.107273.

Shi, X., Li, D., Deng, Q., Peng, Z., Zhao, C., Li, Xiaobing, Wang, Z., Li, Xinwei, Liu, G., 2016. Acetoacetic acid induces oxidative stress to inhibit the assembly of very low density lipoprotein in bovine hepatocytes. J. Dairy Res. 83 (4), 442–446. https://doi.org/10.1017/S0022029916000546.

Shmarakov, I.O., Borschovetska, V.L., Blaner, W.S., 2017. Hepatic detoxification of bisphenol a is retinoid-dependent. Toxicol. Sci. 157 (1), 141–155. https://doi.org/10.1093/toxsci/kfx022.

Sriram, K., Benkovic, S.A., Hebert, M.A., Miller, D.B., O'Callaghan, J.P., 2004. Induction of gp130-relatedcytokines and activation of JAK2/STAT3 pathway in astrocytes precedes up-regulation of glial fibrillary acidic protein in the 1-methyl-4-phenyl-1,2,3,6-tetrahydropyridine model of neurodegeneration: key signaling pathway for ast. J. Biol. Chem. 279, 19936–19947. https://doi.org/10.1074/jbc.M309304200.

Stevens, C.S., Rosado, H., Harvey, R.J., Taylor, P.W., 2015. Epicatechin gallate, a naturally occurring polyphenol, alters the course of infection with β-lactam-resistant Staphylococcus aureus in the zebrafish embryo. Front. Microbiol. 6, 1043. https://doi.org/10.3389/FMICB.2015.01043.

Sun, S.X., Zhang, Y.N., Lu, D.L., Wang, W.L., Limbu, S.M., Chen, L.Q., Zhang, M.L., Du, Z. Y., 2019. Concentration-dependent effects of 17β-estradiol and bisphenol A on lipid deposition, inflammation and antioxidant response in male zebrafish (Danio rerio). Chemosphere 237, 124422. https://doi.org/10.1016/j.chemosphere.2019.124422.

Thoene, M., Rytel, L., Dzika, E., Włodarczyk, A., Kruminis-Kaszkiel, E., Konrad, P., Wojtkiewicz, J., 2017. Bisphenol A causes liver damage and selectively alters the neurochemical coding of intrahepatic parasympathetic nerves in juvenile porcine models under physiological conditions. Int. J. Mol. Sci. 18 (12), 2726. https://doi.org/10.3390/ijms18122726.

Tian, S., Yan, S., Meng, Z., Huang, S., Sun, W., Jia, M., Teng, M., Zhou, Z., Zhu, W., 2021. New insights into bisphenols induced obesity in zebrafish (Danio rerio): activation of cannabinoid receptor CB1. J. Hazard. Mater. 418, 126100 https://doi.org/10.1016/J.JHAZMAT.2021.126100.

Tripathi, A., Debelius, J., Brenner, D.A., Karin, M., Loomba, R., Schnabl, B., Knight, R., 2018. The gut-liver axis and the intersection with the microbiome. Nat. Rev. Gastroenterol. Hepatol. 15 (7), 397–411. https://doi.org/10.1038/S41575-018-0011-Z.

Waheed, Z., Choudhary, J., Jatala, F.H., Fatimah, Noor, A., Zerr, I., Zafar, S., 2023. The role of tau proteoforms in health and disease. Mol. Neurobiol. 60, 5155–5166. https://doi.org/10.1007/S12035-023-03387-8.

Wang, K., Qiu, L., Zhu, J., Sun, Q., Qu, W., Yu, Y., Zhao, Z., Shao, G., 2021. Environmental contaminant BPA causes intestinal damage by disrupting cellular repair and injury homeostasis in vivo and in vitro. Biomed. Pharmacother. 137, 111270 https://doi.org/10.1016/J.BIOPHA.2021.111270.

Wang, L., Wang, B., Hu, C., Wang, C., Gao, C., Jiang, H., Yan, Y., 2023. Influences of chronic copper exposure on intestinal histology, antioxidative and immune status, and transcriptomic response in freshwater grouper (Acrossocheilus fasciatus). Fish Shellfish Immunol. 139, 108861 https://doi.org/10.1016/J.FSI.2023.108861.

Zang, L., Ma, Y., Huang, W., Ling, Y., Sun, L., Wang, X., Zeng, A., Dahlgren, R.A., Wang, C., Wang, H., 2019. Dietary lactobacillus plantarum ST-III alleviates the toxic effects of triclosan on zebrafish (Danio rerio) via gut microbiota modulation. Fish Shellfish Immunol. 84, 1157–1169. https://doi.org/10.1016/j.fsi.2018.11.007.

Zhao, F., Jiang, G., Wei, P., Wang, H., Ru, S., 2018. Bisphenol S exposure impairs glucose homeostasis in male zebrafish (Danio rerio). Ecotoxicol. Environ. Saf. 147, 794–802. https://doi.org/10.1016/J.ECOENV.2017.09.048.

Zhu, Z., Long, X., Wang, J., Cao, Q., Yang, H., Zhang, Y., 2023. Bisphenol A has a sex-dependent disruptive effect on hepatic lipid metabolism in zebrafish. Comp. Biochem. Physiol. Part C Toxicol. Pharmacol. 268, 109616 https://doi.org/10.1016/J.CBPC.2023.109616.